Journal of Molecular Structure 1106 (2016) 200–209

Contents lists available at ScienceDirect

Journal of Molecular Structure

journal homepage: http://www.elsevier.com/locate/molstruc

Structural and chiroptical analysis of naturally occurring (−)-strychnine

F. Reinscheid [a], M. Schmidt [a], H. Abromeit [b], S. Liening [b], G.K.E. Scriba [b], U.M. Reinscheid [a, *]

[a] NMR-based Structural Biology, Max-Planck-Institute of Biophysical Chemistry, Am Fassberg 11, 37077 Göttingen, Germany
[b] Pharmaceutical Chemistry, Friedrich-Schiller Universität, Philosophenweg 14, 07743 Jena, Germany

ARTICLE INFO

Article history:
Received 10 July 2015
Received in revised form
15 September 2015
Accepted 19 October 2015
Available online 23 October 2015

Keywords:
Strychnine
Structure
NMR
Optical rotation
Electronic circular dichroism
Conformation

ABSTRACT

Structural aspects such as chemical exchange, dimerization, solvent association, nitrogen inversion and protonation status of strychnine were investigated using experimental and calculated data. The information was mainly interpreted in view of a successful determination of the absolute configuration (AC) with strychnine (base and salt) as test molecule due to its importance in chemistry. By geometry optimization a stable isomer of protonated strychnine was found with an inverted nitrogen, however, 25 kcal/mol higher in energy. It is shown that solvent association can be assumed in protic solvents such as methanol and dimerization to a small extent in polar/protic solvents. However, the monomeric structural model neglecting explicit solvent molecules still allows the correct prediction of the AC of base and hydrochloride using optical rotation and ECD data.

1. Introduction

Recently, it was stated that "today the focus of chemical research is much more on function than on structure." [1] Although it is still more difficult to give answers to functional questions on the same scientific level as has been achieved for structural research, it is important to push the limits in structural descriptions even further. Since a number of stereochemical misassignments of natural products can be found in the literature (for reviews) [2–5], studying the structure of known molecules may give surprising results. Two recent examples are the correct determination of the absolute configuration (AC) of the antimalarial drug mefloquine [6], and the discovery of the yet hidden structural flexibility of strychnine [7]. Even this extremely well studied (first isolation in 1818 by Pelletier and Caventou) [8] prototypic molecule of rigidity turned out to exist as two conformers in solution. Consequently, all functional effects due to the presence of a minor conformer will be neglected if only the crystal structure of strychnine [9,10] is considered.

The structure of strychnine (Scheme 1) has been established by Robinson [11]. Soon after it was confirmed by total synthesis [12] and x-ray crystallography [13]. The absolute configuration of naturally occurring (−)-strychnine was determined by Peerdeman in 1956 using x-ray crystallography [14]. Apart from the general chemical importance of strychnine, there is an astonishing funnel effect in all synthetic schemes published so far: either the Wieland-Gumlich aldehyde is prepared, or isostrychnine [15,16]. From these intermediates known conversions lead to strychnine, but are quite often not performed. In addition, comparing the IR spectra presented as proof for the successful synthesis of strychnine [17] leads to the conclusion that two identical spectra are shown. To the best of our knowledge, the only further structural information concerning the conversion of isostrychnine into strychnine [18] was given by Magnus et al. [19] in their introduction to the second total synthesis of strychnine, more than 30 years after Woodward's first total synthesis. Magnus et al. [19] mentioned without giving experimental details, that by using different reaction conditions as Prelog et al. [18], i.e. ethanolic potassium hydroxide at 80 °C, almost no conversion into strychnine was observed, and in case of cesium carbonate in *tert*-butyl alcohol as solvent 13-*epi*-isostrychnine was formed. In conclusion, the strychnine chemistry is far from being well understood. This motivated us to further analyse experimentally and computationally the structural model of strychnine,

* Corresponding author.
E-mail address: urei@nmr.mpibpc.mpg.de (U.M. Reinscheid).

http://dx.doi.org/10.1016/j.molstruc.2015.10.062
0022-2860/

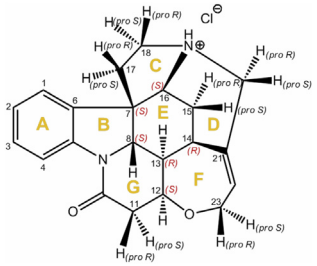

Scheme 1. Stereochemical formula of (−)-strychnine HCl.

followed by a chiroptical analysis. Insofar serves strychnine as a test molecule to explore the success and limitations of the purely chiroptical approach to determine the AC of a chiral compound.

2. Results and discussion

2.1. Structural model

In our first publication about the structure of strychnine, we showed the first experimental and quantitative evidence of a minor conformer in solution using low-temperature NMR (Fig. 1) [7a]. Structure calculation of this low-populated conformer is successful on the mpw1pw91/cc-pvdz level of theory, but not on the often used B3LYP/6-31G(d) level of theory [7a]. Earlier work by Butts et al. (2011) [7b] presented calculated quantitative information. In addition, a third low-populated conformer was predicted by computation [52]. To date, there is no experimental evidence for its existence so it was not further investigated.

In the present study we investigate structural aspects in order to explore the success and limitations of the determination of the absolute configuration by comparing experimental and calculated chiroptical data. Strychnine represents an excellent test molecule for the structural work since it is still a challenging synthetic target and a typically complex natural product. From our analysis we want to derive limits that can be further tested and maybe pushed even further by using smaller natural products such as limonene [20].

2.2. Chemical exchange in ring G

The protons at C11 of strychnine are acidic. It is known that under alkaline conditions these protons can be exchanged by tritiated water [21]. At a hydroxide concentration of 0.1 M, the exchange rate amounts to 4.32×10^4 s^{-1}. However, without using a large excess of hydroxide anions the rate rapidly drops to very small values so that under the conditions of our NMR measurements (measurement times of hours, strychnine at low concentrations of <20 mM, 25 °C (pH of 9.5 (base in water) and pH of 5.5 (strychnine sulphate in water) as saturated solutions) [22] almost no exchange will take place so that the experimental, structural data are not contaminated by fast exchange of the H11 protons. However, this reaction is important for the isostrychnine-strychnine conversion [18]. Likewise, a lactamization reaction is much too slow to produce ring-opened derivatives during the measurements [23], but could be relevant for the isostrychnine-strychnine conversion.

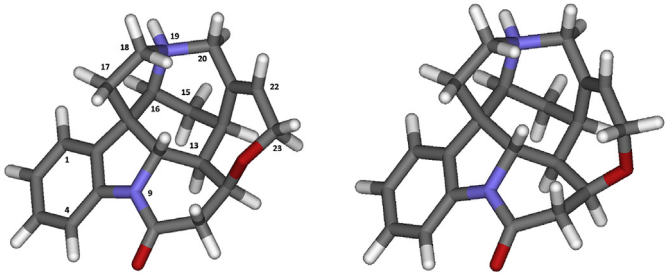

Fig. 1. Geometry-optimized (mpw1pw91/cc-pvdz, IEFPCM: methanol) structure of protonated strychnine (major conformer on the left, minor conformer on the right with a population of 5.9% of strychnine HCl in methanol at 298 K) [7].

2.3. Dimerization, ion-pairing

Mostad [9] analyzed strychnine base by x-ray crystallography. He concluded that the amide oxygen is mostly involved in the intermolecular interactions in the crystal. In order to test the dimerization of (−)-strychnine base, two samples with different concentrations were compared: 2 mg/mL (6 mM) and 100 mg/mL (300 mM) in $CDCl_3$ at 298 K. The proton spectra showed concentration dependent resonances affecting the protons near the aliphatic amine with an upfield shift of more than 0.1 ppm for the high concentration compared to the low concentration, i.e. H16, H18 pro*S*, H20 pro*R* and pro*S*, and H22, located on one side of the 3D-model (Fig. 1; see Supporting information). These data indicate aggregation. In contrast with our results, Metaxas and Cort [24] did not observe concentration dependent effects for the base in chloroform. However, the concentration range studied might be too small so that weak associations were not detected. Assuming a low association constant of 1 $[M]^{-1}$, 6% of the strychnine base molecules would exist as dimer in our high concentration sample (100 mg/mL, 300 mM). For comparison, with an association constant of 100 M^{-1}, 12% of the strychnine base molecules would exist as dimers in our low concentration sample.

For salts of strychnine a concentration dependent change of proton chemical shifts of protons near the protonated tertiary amine were observed (maximum of −8.7 ppb/mM for one of the H20 protons of (−)-strychnine nitrate in $CDCl_3$) [24]. Interestingly, in the same solvent counter-ion dependent proton chemical shifts near the aliphatic nitrogen varied up to 0.3 ppm which can be explained by different ion-pairs formed. Since we have measured strychnine HCl in much more polar and H-bond accepting solvents (DMSO-*d6* and methanol-*d3*), ion-pair formation should be decreased compared to $CDCl_3$, and concomitantly the tendency to form ionic aggregates would be reduced. In agreement, Moreno et al. [25] observed ion-pairing for brucine BF_4 in chloroform which decreased in acetone-*d6* at a 2 mM concentration. With larger anions, strong ion-pairing was observed even in acetone as polar solvent so that we can assume that for strychnine HCl a reduced ion-pairing is reasonable due to the smaller size of the chloride anion compared to $BF4^-$. In agreement, by comparing two samples 2 mg/mL (5 mM) and 65 mg/mL (163 mM) in methanol-*d3* at 298 K, we observed that the protons surrounding the aliphatic nitrogen are mostly affected but to a lower extent compared to the base in chloroform, i.e. H15 pro*R*, H16, H17 pro*R*, H18 pro*S* by more than 0.03 ppm (see Supporting information). In this case, up- and downfield shifts were observed. Interestingly, H1 at the aromatic ring is shifted by 0.04 ppm downfield at the higher concentration. These concentration dependent differences in chemical shifts are smaller than the values observed by Metaxas and Cort [24] due to the different solvent effect on the aggregation/ion-pairing process. The latter is much more pronounced in apolar solvents such as chloroform used by Metaxas and Cort [24] compared to the polar solvent methanol-*d3* in our study. In conclusion, there are clear indications of aggregation of strychnine base (in $CDCl_3$) and strychnine HCl (in methanol-*d3*) at very high concentrations. It is therefore reasonable to use a monomer as structural model if the chiroptical analysis is performed at sufficiently low concentrations, i.e. <20 mM. In polar solvents and at low concentrations of

strychnine HCl, the effect of ion-pairing on the chiroptical analysis can be neglected.

2.4. Solvent-association

Strychnine contains six potential H-bond accepting (HBA) sites: the amine and amide nitrogens, the amide and ether oxygens, and the ethylene and benzene moieties [26]. The authors analysed IR spectra of 4-fluorophenol as H-bond donor together with strychnine and observed 3 OH bands. This indicated that three sites are preferred, in the following order of decreasing basicity: aliphatic amine (N19), O-amide, and O-ether. To study such solvent-associations ^{15}N chemical shifts are very important parameters. In addition, they might indicate the protonation state [27], dimerization, and the presence of ion-pairs. The latter information was already utilized for the determination of the absolute configuration of mefloquine HCl in DMSO [6].

In addition, the comparison between calculated and experimental ^{15}N resonances is a valuable tool to construct the structural model [28–30]. Ramalho and Bühl [29] showed that the ^{15}N chemical shifts of the references such as nitromethane are highly dependent on the level of theory. We propose to use an internal referencing to circumvent this dependence on the level of theory. As an example, taking the calculated data for 5-nitroimidazole using DFT and the PCM approach to model solvent effects, the absolute difference between the two nitrogen resonances was 97 ppm (BP86 functional, DMSO as solvent for geometry optimization and NMR calculation) which is very close to the experimental difference of 96.8 ppm [29]. A different approach used empirical solvent scales such as the normalized solvent polarity scale of Reichardt in order to obtain a good correlation for the ^{15}N chemical shifts of pyrimidine [31]. In addition, by scaling of the spheres (standard value of 1.2) used within the PCM approach to define the cavity a better match to experiment for pyrimidine in water was achieved using a value of 1.1 [32].

Solvent effects on tertiary amine resonances are dominated by hydrogen bonding to the lone pair of the nitrogen, resulting in downfield shifts [30,33]. For *N*-methylpiperidine, the nitrogen resonance was shifted downfield in chloroform as solvent by 3 ppm and 2.4 ppm compared to cyclohexane for chloroform and methanol, respectively [33]. In addition, H-bonding of chloroform to acetamide was measured [34]. Association constants of 0.46 M^{-1} for *N*-methylacetamide and 0.99 M^{-1} for *N*,*N*-dimethylacetamide were found at 16 °C. Similar values were determined by Wong and Ng [35] for tertiary amines and ethers (e.g. 0.45 M^{-1} for tetrahydrofurane at 34 °C) as H-bond acceptors with chloroform as proton donor so that solvent association with strychnine is expected for the tertiary aliphatic N19, the amide group and the ether linkage in ring F.

From these literature values one would expect downfield shifts when going from DMSO-*d6* to $CDCl_3$ for the two nitrogen resonances of strychnine base due to H-bonding, in contrast to the experiment (Table 1). Obviously, other effects such as solvent polarity and/or H-bonding to other parts of the molecule are relevant. In addition, using the referencing between the two nitrogen resonances, the experimental (DMSO-*d6*/$CDCl_3$) and calculated differences (113 ppm/115 ppm and 119.8 ppm, respectively, Table 1) differ by almost 7 ppm. This indicates that the structural model of isolated strychnine base does not fully represent the measurement conditions and/or that the calculations are erroneous. The difference between the two nitrogen resonances changed dependent on the level of theory by 3.9 ppm (mpw1pw91/cc-pvdz vs. mpw1pw91/6-311 + g(d,p)) and by 1.7 ppm (B3LYP/cc-pvdz vs. mpw1pw91/cc-pvdz) so that computational errors are one of the reasons for the large discrepancies between experiment and calculation.

Similar to strychnine base, the experimental (DMSO-*d6*/methanol-*d3*) and calculated differences for strychnine HCl/protonated strychnine differ (87 ppm/89.2 ppm and 92.2 ppm, respectively, Table 1) which might also be related to a systematic error in the calculations.

The proton resonances of strychnine HCl are all shifted downfield in methanol compared to DMSO as solvent for similar concentrations (65 mg/mL in methanol-*d3* and 36 mg/mL in DMSO-*d6*), except the NH proton which is shifted upfield by 1.31 ppm. The interaction area around the aliphatic nitrogen is mostly affected, i.e. H17 pro*S*, H18 pro*S* and pro*R*, and H20 pro*R* are shifted by more than 0.15 ppm (Fig. 1). The ^{13}C resonances follow the same solvent dependence found for the proton values. The chemical shifts appear always downfield in methanol compared to DMSO, with C4, C13, C16, C18, and C20 mostly affected by more than 1.5 ppm chemical shift differences. Apart from the obvious interaction area around the aliphatic nitrogen, there is a downfield shift difference of 1.9 ppm for the carbonyl ^{13}C resonance in methanol compared to DMSO.

In conclusion, it is clear that a substantial fraction of strychnine should exist as solute-solvent complex via the amine, amide and ether functionalities. Without further structural and quantitative information it is not reasonable to construct a static model so that we decided to use an isolated strychnine molecule for the subsequent chiroptical analysis.

2.5. Protonation

The structural model for protonation of tertiary amines may be more complicated than expected. Nagy et al. [37] analyzed theoretically and experimentally the prototypic *N*-methylpiperazine hydrochloride in aqueous solution. Modelling as a monomer could not reproduce the proton NMR-based experimental population analysis. However, as an ionic aggregate composed of one or two chloride anion(s) H-bonded to the organic molecule the calculated results fit very well to the experimental results. In addition, the protonation of the neurotransmitter serotonin reduced the number of low-energy conformers determined by IR spectroscopy and DFT calculations [38] similar to the results of mefloquine HCl [6].

Protonation of tertiary amines typically leads to a downfield shift of ^{15}N resonances (*N*-methylpiperidine HCl in DMSO: 8 ppm downfield of the base in cyclohexane) [33]. This is exactly what was measured for strychnine: protonation of the aliphatic nitrogen shifts the ^{15}N resonance 25–30 ppm downfield (Table 1). The much larger difference between the two ^{15}N resonances for the basic compared to the protonated state (115/113 ppm to 89.2/87 ppm) is correctly reproduced by the calculations (119.8–92.2 ppm). The difference (N9–N19) upon protonation is 28 ppm for experiment (DMSO-*d6*, base-HCl: 115 ppm–87 ppm) matching very well the calculated value of 27.6 ppm (base/chloroform – protonated/DMSO: 119.8 ppm–92.2 ppm). To conclude, a reasonable model for samples of strychnine HCl in DMSO or methanol shows a protonation at N19.

2.6. Nitrogen inversion

Nitrogen pyramidal inversion means moving the lone pair from one side of the tetrahedral amine to the other. The energy barriers for nitrogen inversion in acyclic amines are in the order of 6–7 kcal/mol [39]. The barrier is increased by hydrogen-bonding [40], protonation [41], and ring formation. Well studied examples are the aziridines for which the barriers of inversion increase up to 18–20 kcal/mol. Substitutions by aromatic rings lower the barrier. As recent example, an aziridine derivative with a cyanophenyl *N*-

Table 1
Experimental and calculated ^{15}N resonances in ppm for strychnine base and strychnine HCl/protonated strychnine in different solvents at 298 K.

^{15}N resonance/Exp. or calc.	N9[a] (δ or σ)	N19[b] (δ or σ)	Absolute difference Δ (N9–N19)
Exp. strychnine HCl in DMSO-*d6* (36 mg/mL)	δ = 150	δ = 63	87
Exp. strychnine HCl in methanol-*d3* (65 mg/mL)	δ = 151.4	δ = 62.2	89.2
Calc. protonated strychnine, DMSO as solvent[c]	σ = 78.6	σ = 170.8	92.2
Exp. strychnine base in DMSO-*d6*[d] (5 mg/mL)	δ = 152	δ = 37	115
Exp. strychnine base in $CDCl_3$ (33 mg/mL)	δ = 148	δ = 35	113
Calc. strychnine base, chloroform as solvent[c]	σ = 101.9	σ = 221.7	119.8

[a] N9: amide nitrogen.
[b] N19: aliphatic nitrogen.
[c] All calculations using DFT on the mpw1pw91/cc-pvdz level of theory, with IEFPCM as solvent model and solvents indicated in the table.
[d] Taken from Hilton and Martin [36].

substitution showed a free energy barrier of 11.3 kcal/mol [42]. The barrier of inversion for *N*-methylpiperidine as example of a larger *N*-heterocyle amounts to 12.0 kcal/mol, which can be further lowererd by α,α-dimethyl substitution. In this case, the crowding is responsible for an increased inversion rate. Belostotskii et al. [43] have analysed the pathways for conformational exchange of piperidines. Following these schemes it appears that literature values must be cautiously interpreted. The authors concluded that the isolated C–N rotation analysed by Anderson et al. [44] is in fact a combination of ring-inversion/nitrogen-inversion, ring-inversion, and isolated C–N rotation. However, a forcefield (MM3) based scheme was applied so that shortcomings due to the low level of theory were not taken into account [43].

Two interconverting species separated by a barrier larger than 23 kcal/mol corresponding to a transition rate of less than 10^{-4} s^{-1} can be separated [45]. This means that very often nitrogen-inverted isomers cannot be separated and explains how scarce data about these isomers are, although a large number of bioactive compounds and pharmaceuticals contains tetrahedral amines. The speed of the inversion process often hinders the direct measurement in solution by NMR. Quite often, enantiotopic groups in α position to the nitrogen are used for the analysis. An interesting example for slowing down the process is the complexation by supramolecular host molecules [46].

Among the most fascinating natural products, cocaine plays a special role since it is the most abused bioactive compound worldwide. Interestingly, Poupaert et al. [47] reported a nitrogen inversion of the tertiary amine of cocaine that is highly dependent on the solvent: the form with an intramolecular H-bond is favoured in CD_2Cl_2 whereas in water the form with a solvent-directed proton is dominating [48]. However, the inversion barrier was calculated on quite low levels of theory so that the two energies (AM1: 7.9 kcal/mol; PM3: 6.7 kcal/mol) can only be taken as rough estimates [47]. Furthermore, experiments are needed with specified concentrations and pH conditions since these parameters are also relevant for the observed inversion rate. The latter point seems to be relevant for the investigation about trimipramine maleate [49]. The authors interpreted the results as nitrogen inversion with a barrier of 16.3 kcal/mol. This value is very high for an aliphatic dimethylamino group. Since also concentration effects were observed, a careful interpretation of the low temperature spectra is very important. Increasing the concentration led to an apparent increase of the inversion rate. This can be an artifact if aggregates with smaller chemical shift differences are formed. In addition, the pH influences heavily the apparent inversion rate since only the basic form can exhibit nitrogen inversion.

Protonation further slows down the inversion since deprotonated forms are the only species that are able to invert [50]. Therefore, the protonation state is very important since it influences the observed rate of inversion. The aliphatic nitrogen of strychnine is more basic compared to the amide nitrogen so that strychnine salts will have a protonated aliphatic nitrogen (pK_A values of 6.0 and 11.7 at 20 °C; pH of a saturated solution of strychnine base: 9.5; pH of a saturated strychnine sulphate solution: 5.5 [22]. In their analysis, Morgan and Leyden [50] could show that the concentration of the base might also influence the inversion rate. However, in the case of strychnine, the concentrations in the NMR measurements were quite low (<20 mM). This means that too few strychnine molecules were available as base to assist the deprotonation of a protonated strychnine molecule. Consequently, in methanol and DMSO we expect that solvent assisted deprotonation is the major process, maybe with the counter-ions as acceptors as illustrated in the following.

Rates of proton exchange for the hydrochloride of *N*,*N*-dibenzylaniline were measured in $CDCl_3$ and acetonitrile-*d3* [51]. Importantly, small amounts of water in $CDCl_3$ with an at least 30-fold excess of test compound did not change the exchange rates. Likewise, the concentration of the test compound did not affect the proton exchange rate. Very similar free energies of activation were obtained for acetonitrile. However, this appeared to be caused by an enthalpy-entropy compensation. Interestingly, the authors conclude that the chloride anion acts as proton acceptor since water and amine as base could be excluded. This is in agreement with the observations of Metaxas and Cort [24] who found strong influences of the counter-ions on the proton resonances of strychnine salts.

By geometry optimizations we detected a second minimum for the protonated (−)-strychnine conformers belonging to an inverted aliphatic nitrogen stereoisomer (Fig. 2). The free energy difference on the mpw1pw91/cc-pvdz (IEFPCM with methanol) level of theory was quite large (25.1 kcal/mol for the major conformer and 29.2 kcal/mol for the minor conformer) which can be explained by the highly strained ring systems in which the amine is involved. The envelope of the five-membered ring C is changed (*endo* position of C7 in the non-inverted forms of Fig. 1; *endo* position of N19 in the inverted forms in Fig. 2). Interestingly, the boat form of ring D

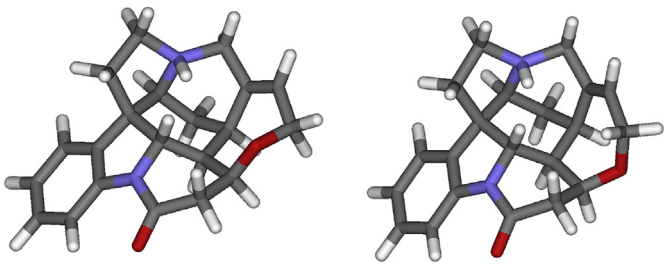

Fig. 2. Geometry-optimized (mpw1pw91/cc-pvdz, IEFPCM: methanol) structure of protonated strychnine with inverted aliphatic nitrogen (major conformer on the left, minor conformer on the right with a population of 2.7% of strychnine base in chloroform at 298 K) [7].

remains very similar. We could not find a minimum for the nitrogen-inverted strychnine base. From the Boltzmann-derived populations it is clear that the nitrogen inversion of the aliphatic amine in protonated strychnine was not detected at low temperatures (210 K, methanol-*d3*) [7] due to the low population of the inverted form.

However, synthetic reactions might create conditions under which nitrogen inversion occurs much faster and/or the inverted isomer dominates. One prominent example could be the isostrychnine-strychnine conversion performed at high pH. This leads to a high concentration of strychnine as base. In addition, it would be interesting to analyze nitrogen-inversion for strychnine isomers. Bifulco et al. [52] showed that it is possible to determine the relative configuration of naturally occurring strychnine by comparing the experimental $^{1}J_{CC}$ couplings with calculated ones of all possible diastereomers. However, isomers with inverted nitrogen were not yet taken into account.

2.7. Optical rotatory dispersion

The Sigma–Aldrich product information about the specific optical rotation of (−)-strychnine base is [α] = −139.0 at 22 °C, c = 1 in chloroform (1.0 g compound dissolved in 100 mL of solvent which equals 10 mg/mL) at a wavelength of 589 nm. The sulphate showed a specific optical rotation at 25 °C and 589 nm of −25.1 [22]. For the hydrochloride (7 mg/mL in water at 25 °C) a specific rotation of −28.3 at 589 nm is reported [53]. We measured in chloroform at 24.5 °C a specific optical rotation [α] = −141 for strychnine base (589 nm, c = 20 mg/mL, i.e. c = 2) which differs by less than 2% from the Sigma–Aldrich product information. The strychnine HCl measurement of [α] at 24.5 °C (c = 2, methanol as solvent) gave −15 at 589 nm. The difference to the literature value might be explained by a solvent dependence of [α].

Using the aug-cc-pvdz basis set, we achieved to predict correctly the AC of strychnine base (Fig. 3) and strychnine HCl (Fig. 4) by comparing calculated with experimental values. Values of (−)-strychnine HCl were corrected for a protonated form for comparison with the calculated values obtained with a protonated structural model. Figs. 3 and 4 show that the minor conformer [7a] only slightly contributes to the calculated ORD values (mpw1pw91/aug-cc-pvdz, IEFPCM solvent model with methanol (protonated strychnine) or chloroform (strychnine base) as solvent) since the ORD values are quite small or similar compared to the major conformer.

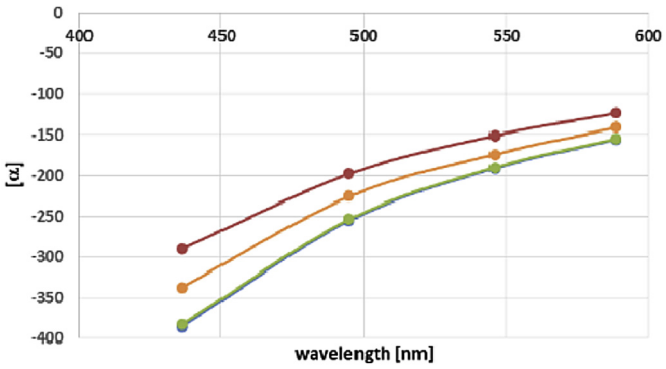

Fig. 3. Calculated (mpw1pw91/aug-cc-pvdz, iefpcm: chloroform; in blue partly overlaid by the green curve: major conformer, in red: minor conformer, in green: 97.3/2.7 mix of the two conformers) and experimental (in orange, 2% in chloroform) ORD curve of (−)-strychnine base based on four wavelengths (589, 546, 495, and 436 nm respectively).

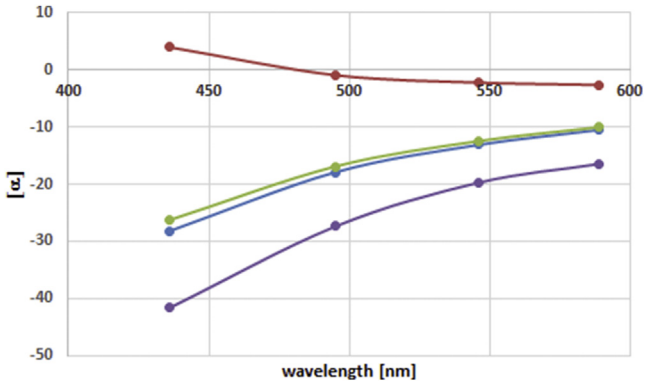

Fig. 4. Calculated (mpw1pw91/aug-cc-pvdz, iefpcm: methanol; in blue: major conformer, in red: minor conformer, in green: 94.1/5.9 mix of the two conformers) and experimental (in purple, 2% in methanol) ORD curve of (−)-strychnine HCl/protonated strychnine based on four wavelengths (589, 546, 495, and 436 nm respectively).

The experimental values shown are measured at a quite high concentration (2%) but are still low enough to be modelled by a monomeric isolated molecule. Values obtained for a concentration of 0.2% together with the values for 2% are shown in Table 2. A dependence on the concentration was observed which was ascribed to the limited precision of the polarimeter (α ± 0.01) which translates to [α] changes of ±20 in our measurements using the lowest concentration of 0.2%. In addition, from our structural analysis it is clear that aggregation and solvent-solute interactions are present at high concentrations but are neglected in our structural model. However, since no sign changes occurred at all concentrations and wavelengths measured, a monosignate behaviour of the ORD curve was safely determined for which a much better AC prediction can be obtained compared to the single value optical rotation at 589 nm [54].

In view of an uncertainty of roughly ± 60 for the calculation of $[\alpha]_D$ [55], the AC prediction of strychnine (base and hydrochloride) should be based on several wavelengths. It is important to note that even with the inclusion of solvent effects and zero-point vibrational corrections, a number of signs of the optical rotation of (*S*)-propylene oxide were not predicted correctly so that further shortcomings of the procedure (e.g. level of theory, dynamic effects in condensed phases) must exist [56]. However, we expect a higher precision than the above mentioned range of values due to the improvement achieved in the calculations of chiroptical properties. Especially, inclusion of solvents as dielectric continuum typically improves the match with experiment [57]. Furthermore, the better the structural model, the better the agreement. Only notoriously problematic molecules such as the above mentioned (*S*)-propylene oxide still pose severe problems for the AC assignment.

2.8. UV–vis and ECD

In Tables 3 and 4 the experimental molar extinction coefficients are listed for (−)-strychnine base and (−)-strychnine HCl, respectively. There are discrepancies between the experimental and calculated extinction coefficients (Table 5). In principle, the level of theory and the modelling by gaussian bandshapes are two factors that can be responsible for the differences. However, it is clear that there are substantial solvent effects if the strychnine base data in methanol are compared with acetonitrile at similar concentrations. Based on the above mentioned analysis we assume that specific solute-solvent interactions might be responsible for the solvent

Table 2
Experimental specific optical rotation at different wavelengths at two concentrations for (−)-strychnine base (in chloroform) and (−)-strychnine HCl (in methanol).

Wavelength [nm]	[α] of strychnine base 2%	[α] of strychnine base 0.2%	[α] of strychnine HCl 2%	[α] of strychnine HCl 0.2%
589	−141	−110	−15	−40
546	−174	−160	−18	−30
495	−226	−210	−25	−50
436	−338	−310	−38	−40

Table 3
Experimental molar extinction coefficients ε [l M^{-1} cm^{-1}] for (−)-strychnine base in different solvents and different concentrations, all at 25 °C and λ_{max} = 255 nm, except in methanol (λ_{max} = 254 nm).

	$CHCl_3$ (0.049 mg/mL)	$CHCl_3$ (0.47 mg/mL)	Methanol (0.12 mg/mL)	Acetonitrile (0.029 mg/mL)	Acetonitrile (0.145 mg/mL)
ε	7590	11,070	12,420	28,640	28,410

Table 4
Experimental molar extinction coefficients ε [l M^{-1} cm^{-1}] of strychnine HCl in methanol at different concentrations, all at 25 °C and λ_{max} = 255 nm.

	0.378 mg/mL	1.3 mg/mL
ε	9950	11,610

dependent ECD spectra.

The experimental λ_{max} values all appear at 255 nm for strychnine base (except for methanol: 254 nm) which is quite similar to the calculated values (Table 5). For strychnine base in chloroform, a concentration dependent extinction coefficient was determined which might be explained by aggregation and/or solute-solvent interactions. This effect was not observed for strychnine base in acetonitrile and strychnine HCl in methanol, two solvents with much higher polarity.

We concentrate on the comparison between calculated and experimental excitation energies useful for the interpretation of the ECD bands. It is important to note, that we did not apply any scaling to neither wavelengths nor intensities to allow for own interpretations of the reader. In our opinion, the interpretation and comparison of calculated and experimental ECD spectra is problematic if scalings of the wavelength and intensity axis are used. As an example, Shimizu et al. [58] scaled the intensities by a factor of 0.5, fixed the broadening at 0.4 eV, and used different shifts for the wavelength axis (0.3 eV, 0.7 eV red shift, 1.0 eV blue shift) depending on the level of theory. For all three measures, no explicit reasoning was indicated. With respect to our scientific goal to explore the success and the limitations of the prediction of the absolute configuration based on chiroptical data, we cannot recommend this procedure. Especially n−π* transitions are notoriously difficult to predict in solution (see Supporting information for some literature examples).

Snow and Hooker [59] have measured (−)-strychnine in aqueous acidic solution and as a base in triethylphosphate (TEP). Unfortunately, no information was given about the acidifiying agent so that it remains unknown which salt has been formed. Likewise, an aqueous neutral sample was measured but no information was given about its preparation. Additionally, an apparent aggregation at alkaline pH was mentioned but no further information given. In the UV spectrum of (−)-strychnine two shoulders (287 nm and 277 nm) were identified in the aqueous neutral sample. The following ECD bands together with their signs were measured for aqueous strychnine at pH 3 [59]: 210 nm (−), 250 nm (+); for strychnine in TEP: 205 nm (−), 230 nm shoulder (−), 260 nm (+), 280 nm (−). All bands also appear in our spectra except the band at 205 in TEP, since we have used solvents with a higher wavelength cut-off. The shoulder at 230 nm was tentatively assigned to the n−π* transition of the carbonyl oxygen lone pairs [59]. Two arguments were put forward: 1. the transition seems to be electrically forbidden since no corresponding UV absorption band was detected; 2. such transitions are very sensitive to the environment which was shown for this ECD band for strychnine and five related compounds: it shifts dependent on the solvent and pH. We also detected solvent dependent shifts, notably in acetonitrile strychnine base (Fig. 5E) does not show a positive ECD band around 255 nm which is present in all other solvents (chloroform and methanol) for (−)-strychnine base and in methanol for (−)-strychnine HCl. Calculations indicate that protonation increases the intensity of the positive ECD band around 255 nm. The list of rotational strengths can be found in the Supporting information.

The calculations for (−)-strychnine base clearly show a broad negative ECD band around 250 nm that correlates with the negative band around 235 nm in the experiment (acetonitrile) which is supported by comparison of the experimental and calculated UV spectra (Figs. 5 and 6). Since an incorrect modelling of n−π* transitions is likely, it is important to explore different levels of theory for smaller test molecules [20]. The calculated ECD bands for protonated (−)-strychnine match with experiment without any wavelength shift (Fig. 5F and G; Fig. 6E–H). Interestingly, the calculated ECD bands for the major and minor conformers of strychnine base and protonated strychnine differ slightly. However, the decisive negative band around 250 nm is always present so that the AC assignment is reliable. In conclusion, the good match between experiment and calculation proves that the naturally occurring (−)-strychnine HCl is assigned 13*R* since this was the configuration of the structural model used (Scheme 1). In the case of (−)-strychnine base, higher levels of theory might improve the fit with experiment.

Table 5
Calculated molar extinction coefficients ε [l M^{-1} cm^{-1}] for (−)-strychnine base in chloroform and protonated (−)-strychnine in methanol (mpw1pw91/cc-pvdz, IEFPCM).

	Strychnine base, conformer 1	Strychnine base, conformer 2	Protonated strychnine, conformer 1	Protonated strychnine, conformer 2
ε	14,459	14,571	12,741	12,402
λ_{max} [nm]	247	246	244	244

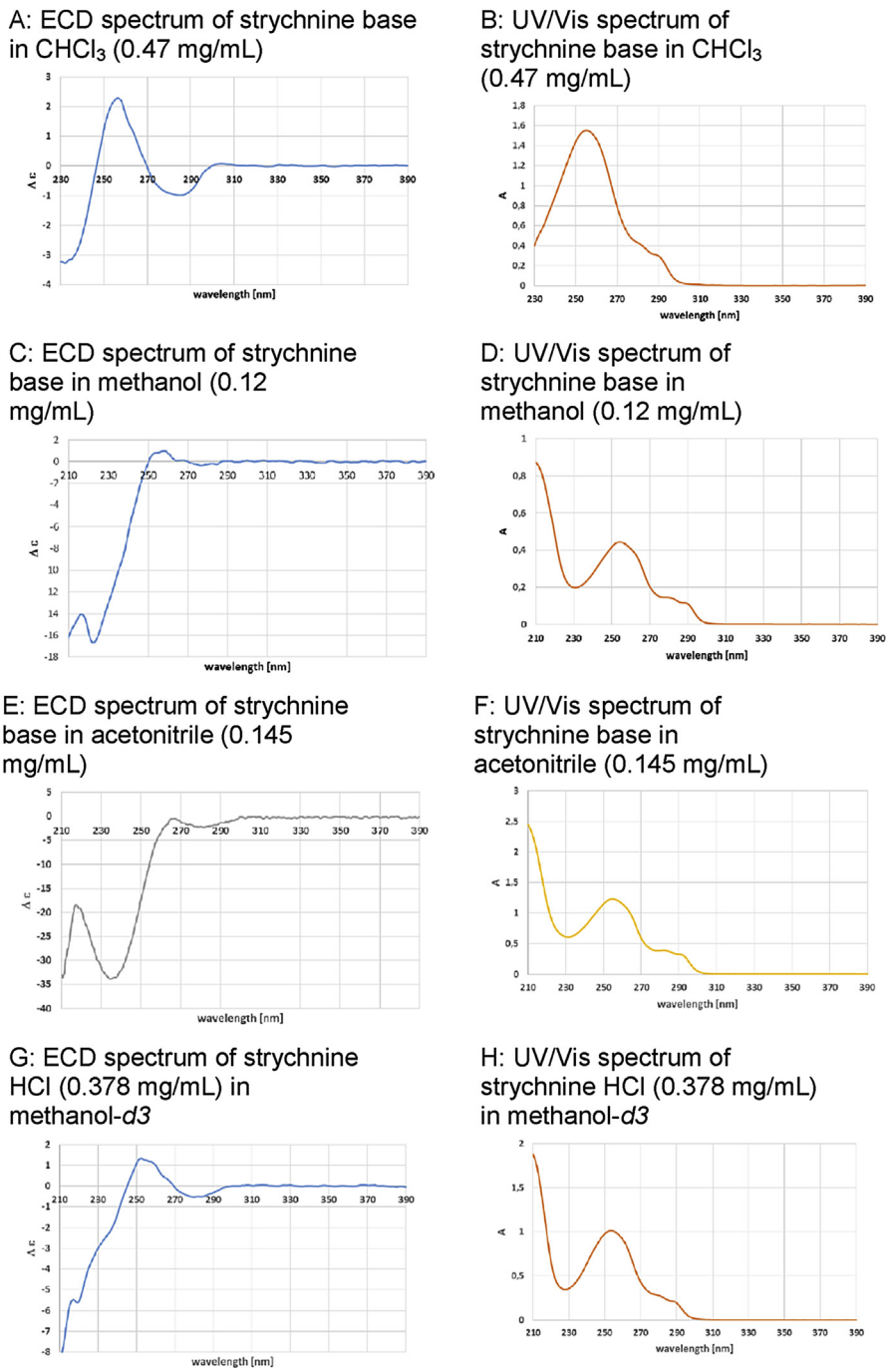

Fig. 5. A–H: Experimental ECD and UV/vis spectra of (−)-strychnine base and (−)-strychnine HCl in different solvents and at different concentrations at 25 °C.

2.9. IR and VCD

Setnička et al. [60] presented IR and VCD spectra of (−)-brucine in three different solvents: $CDCl_3$, methanol-*d3*, and DMSO-*d6*. Under the experimental conditions the AC determination is problematic since very high concentrations (>0.16 M) were used and aggregation has to be taken into account for the structural modelling. Neglecting aggregation effect and assuming that the two methoxy groups of brucine only slightly influence the two selected VCD bands (1660 cm^{-1} and 1500 cm^{-1}), we took the (−)-brucine information for comparison with our calculated (−)-strychnine VCD data. The corresponding IR bands appear in strychnine crystals at 1667 cm^{-1} and 1476 cm^{-1}, judged by the intense intensities [61] so that the band identification should be correct. Only the IR band at higher wavenumbers shows a solvent dependent shift of roughly 20 cm^{-1} at most. Since this band appears isolated in the spectrum, it can be safely assigned as amide stretch. In addition, the corresponding VCD band at 1660 cm^{-1} shows almost no shift in wavenumbers depending on the solvent due to the quite broad absorption bands. The VCD bands have a negative (1660 cm^{-1}; amide stretch) and a positive sign (1500 cm^{-1}). The calculated IR amide band of (−)-strychnine base (major conformer) is shifted by ca. 115 cm^{-1} to higher wavenumbers (1775 cm^{-1}, Fig. 7, top), and the calculated VCD band

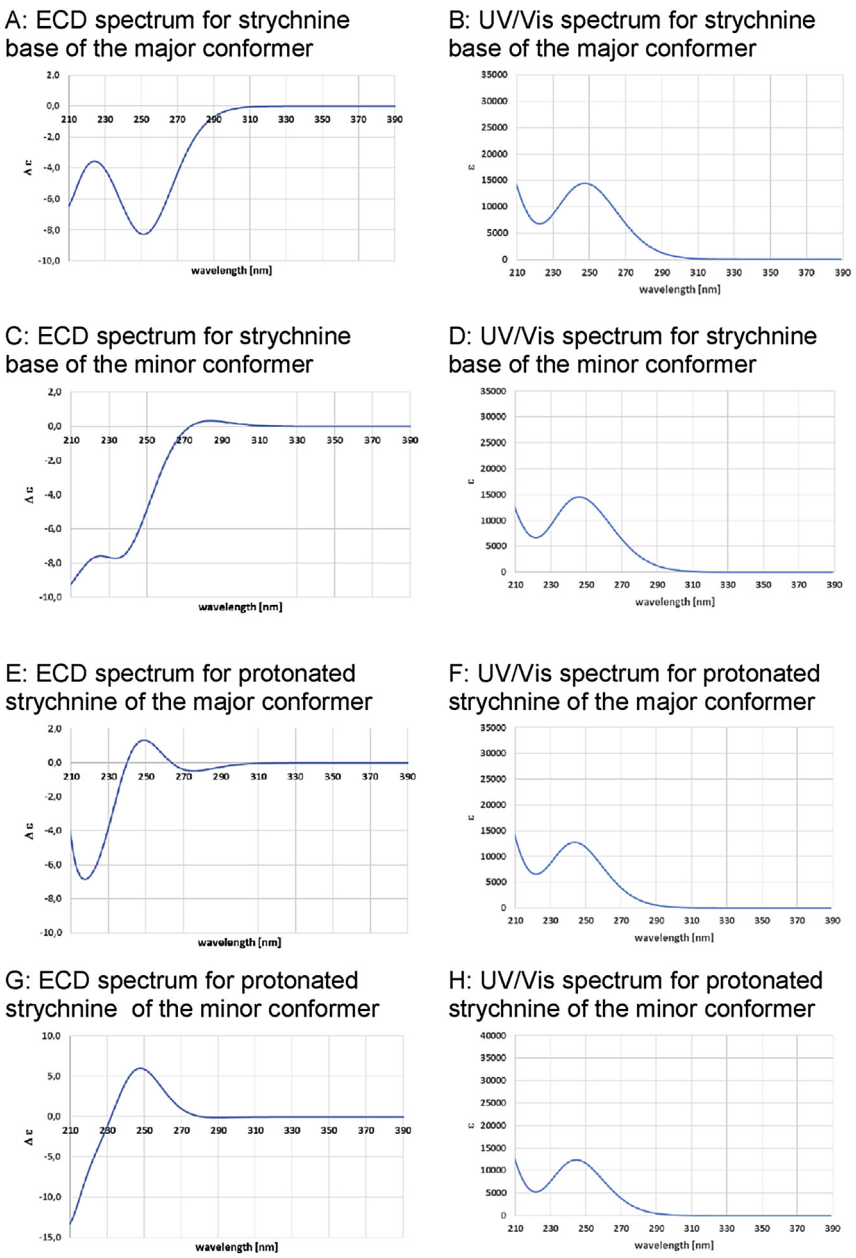

Fig. 6. A–H: Calculated ECD and UV/vis spectra of (−)-strychnine base and protonated (−)-strychnine of the major and minor conformer [7a] at the mpw1pw91/cc-pvdz level of theory using the IEFPCM approach and chloroform (strychnine base) or methanol (protonated strychnine) as solvent.

(major conformer) has a negative sign (Fig. 7, bottom), matching with experiment. The experimental VCD band at 1500 cm^{-1} cannot be reliably assigned in the calculated spectrum. We conclude that applying the VCD amide band of (−)-brucine for (−)-strychnine gives the correct AC assignment for (−)-strychnine (calculated spectra of the minor conformer and of protonated (−)-strychnine can be found in the Supporting information).

3. Conclusions

The structural analysis based on the comparison between experimental and calculated NMR data justified using a monomeric model of strychnine base and as protonated form. The experimental optical rotation data of both forms matched very well to the calculated values whereas the comparison between the experimental and calculated ECD spectrum of strychnine base showed larger discrepancies compared to the protonated/hydrochloride data pair. Application of the mpw1pw91/cc-pvdz (IEFPCM for solvent modelling) level of theory allowed the correct prediction of the AC of strychnine base and hydrochloride based on the comparison between experimental and calculated ORD and ECD data.

4. Experimental section

(−)-Strychnine base and all other chemicals were obtained from Sigma Aldrich Laborchemikalien GmbH (Germany) and were used without further purification. The purity of (−)-strychnine base was corrected for 100% for all measured values assuming that the strychnine content has an enantiomeric excess of 100%. Solvents

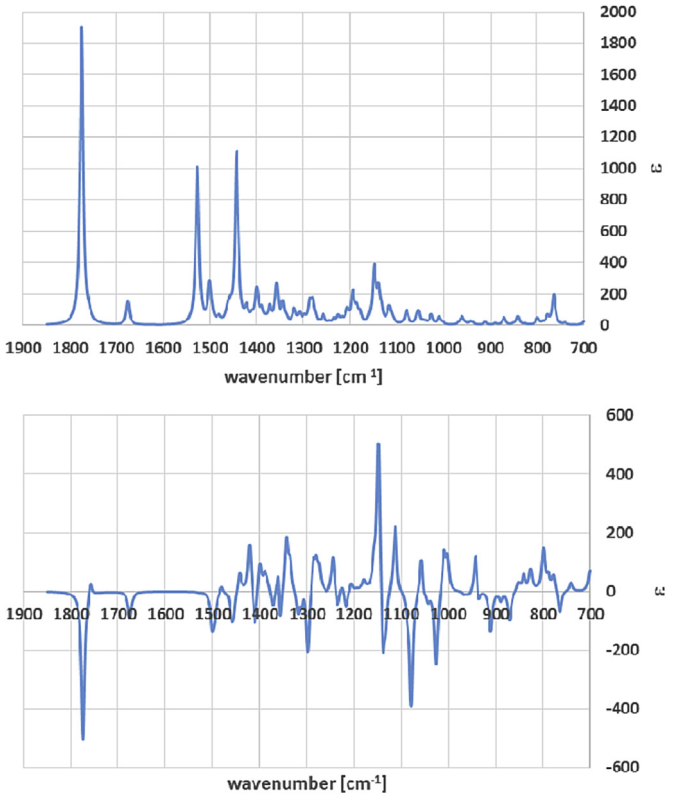

Fig. 7. Calculated spectra of (−)-strychnine base of the major conformer (mpw1pw91/cc-pvdz, IEFPCM: chloroform; IR on top, VCD at the bottom).

had p.a. grade. (−)-Strychnine HCl was formed by dissolving the free base in hydrochloric acid (gas) in ethyl acetate (1.3 M). After precipitation of the strychnine salt the solvent was removed under reduced pressure. The purity was determined by proton NMR and adjusted to 100% for all measured values.

NMR measurements were performed at 298 K using a Bruker Avance 400 MHz NMR spectrometer (400.13 MHz for ^{1}H) equipped with a TXI probe head and a Bruker Avance III 600 MHz NMR spectrometer (600.25 MHz for ^{1}H) equipped with a QXI probe head. The proton spectra were measured for samples of the indicated concentrations with the following parameters: time domain = 32k points, number of scans = 16, apodization with an exponential window function with 0.3 Hz line width, relaxation delay between scans of 2 s.

The UV/vis and ECD spectra were measured using a JASCO J-815 spectrometer and quartz cuvettes with 1 mm path length at 25 °C. Measurement parameter were: scanning speed: 200 nm/min, pitch: 0.5 nm, and band width: 1 nm. All spectra were solvent corrected and represent an average of three consecutive scans. For the ECD spectra values of $\Delta\varepsilon$ [l M^{-1} cm^{-1}] are used. The experimental UV/vis spectra are shown with absorption units.

Optical rotation measurements were performed with methanol or chloroform as solvent at the indicated concentrations using a Polartronic-E polarimeter (Schmidt + Haensch GmbH&Co) at 24.5 °C. The unit of [α] is [degrees*(dm*g/cm^3)$^{-1}$].

5. Computations

For computations G09 and GaussView were used (Gaussian09, RevA.02) [62]. The mpw1pw91 functional [63] was used together with Dunning's correlation consistent basis sets [64,65] for geometry optimization, frequency and IR/VCD calculations, oscillator and rotational strength, specific optical rotation, and chemical shifts. Minima were indicated by the absence of imaginary frequencies. Other levels of theory are indicated in the text. For solvent modelling, the IEFPCM (integral equation formalism polarizable continuum model) approach was applied with the appropriate solvent [57]. IR and VCD spectra were simulated using a broadening of 4 cm^{-1}. The oscillator strengths and rotational strengths were calculated using the velocity representation for the 30 excitations lowest in energy. The calculated UV/vis and ECD spectra were simulated with gaussian bandshapes with a broadening of 0.33 eV. The calculated UV/vis spectra are shown with extinction coefficients ε [l M^{-1} cm^{-1}] on the y-axis.

Acknowledgements

We gratefully acknowledge support by the DFG (FOR 934 to F.R. and U.M.R), the Max-Planck-Society, and by Prof. Griesinger (NMR II, MPIBPC, Göttingen).

Appendix A. Supplementary data

Supplementary data related to this article can be found at http://dx.doi.org/10.1016/j.molstruc.2015.10.062.

References

[1] Royal Swedish Academy of Sciences, 9, Scientific Background on the Nobel Prize in Chemistry 2013, Development of Multiscale Models for Complex Chemical Systems, October 2013.
[2] K.C. Nicolaou, S.A. Snyder, Angew. Chem. Int. Ed. 44 (2005) 1012–1044.
[3] M.E. Maier, Nat. Prod. Rep. 26 (2009) 1105–1124.
[4] M. Elyashberg, A.J. Williams, K. Blinov, Nat. Prod. Rep. 27 (2010) 1296–1328.
[5] T.L. Suyama, W.H. Gerwick, K.L. McPhail, Bioorg. Med. Chem. 19 (2011) 6675–6701.
[6] M. Schmidt, H. Sun, P. Rogne, C. Griesinger, L. Kuhn, U.M. Reinscheid, J. Am. Chem. Soc. 134 (2012) 3080–3083.
[7] a M. Schmidt, F. Reinscheid, H. Sun, H. Abromeit, G.K.E. Scriba, F.D. Sönnichsen, M. John, U. M. Reinscheid, Eur. J. Org. Chem. (2014) 1147–1150;
b C.P. Butts, C.R. Jones, J.N. Harvey, Chem. Commun. 47 (2011) 1193–1195.
[8] P.J. Pelletier, J.B. Caventou, Ann. Chim. Phys. 8 (1818) 323.
[9] A. Mostad, Acta Chem. Scand. B39 (1985) 705–716.
[10] M. Messerschmidt, S. Scheins, P. Luger, Acta Cryst. B61 (2005) 115–121.
[11] R. Robinson, Experientia 2 (1946) 28–29.
[12] R.B. Woodward, M.P. Cava, W.D. Ollis, W.D. Hunger, H.U. Dabniker, K. Schenker, J. Am. Chem. Soc. 76 (1954) 4749–4751.
[13] J.H. Robertson, C.A. Beevers, Nature 165 (1950) 690–691.
[14] A.F. Peerdeman, Acta Cryst. 9 (1956) 824.
[15] J. Bonjoch, D. Solé, Chem. Rev. 100 (2000) 3455–3482.
[16] J.S. Overman, L.E. Cannon, Angew. Chem. Int. Ed. 51 (2012) 4288–4311.
[17] R.B. Woodward, M.P. Cava, W.D. Ollis, W.D. Hunger, H.U. Dabniker, K. Schenker, Tetrahedron 19 (1963) 247–288.
[18] V. Prelog, J. Battegay, W.I. Taylor, Helv. Chim. Acta 30 (1948) 2244–2246.
[19] P. Magnus, M. Giles, R. Bonnert, G. Johnson, L. McQuire, M. Deluca, A. Merritt, C.S. Kim, N. Vicker, J. Am. Chem. Soc. 115 (1993) 8116–8129.
[20] F. Reinscheid, U.M. Reinscheid, J. Mol. Struct. (2015) (accepted).
[21] J.T. Edward, S.C. Wong, A.J. Kresge, M.F. Powell, Can. J. Chem. 62 (1984) 2448–2450.
[22] Muthadi, Hifnawy, Strychnine, Analytical Profiles of Drug Substances, vol. 15, 1986, pp. 563–646.
[23] J.T. Edward, S.C. Wong, R.A. McClelland, Can. J. Chem. 62 (1984) 144–146.
[24] A.E. Metaxas, J.R. Cort, Magn. Reson. Chem. 51 (2013) 292–298.
[25] A. Moreno, P.S. Pregosin, L.F. Veiros, A. Albinati, S. Rizzato, Chem. Eur. J. 15 (2009) 6848–6862.
[26] C. Laurence, M. Berthelot, Perspect. Drug Discov. Des. 18 (2000) 39–60.
[27] U.M. Reinscheid, C. Cychon, M. Köck, V. Schmidts, C. Thiele, C. Griesinger, Eur. J. Org. Chem. 36 (2010) 6900–6903.
[28] S. Chimichi, M. Boccalini, A. Matteucci, S.V. Kharlamov, S. Latypov, O.G. Sinyashin, Magn. Reson. Chem. 48 (2010) 607–613.
[29] T.C. Ramalho, M. Bühl, Magn. Reson. Chem. 43 (2005) 136–146.
[30] G.A. Webb, M. Witanowski, Proc. Indian Acad. Sci. (Chem. Sci.) 94 (1985) 241–290.
[31] V. Manzoni, M.L. Lyra, R.M. Gester, K. Coutinho, S. Canuto, PhysChemChemPhys 12 (2010) 14023–14033.
[32] B. Mennucci, in: S. Canuto (Ed.), Solvation Effects on Molecules and Biomolecules, Springer, 2008, pp. 1–21.
[33] R.O. Duthaler, J.D. Roberts, J. Magn. Reson. 34 (1979) 129–139.
[34] F. Takahashi, N.C. Li, J. Phys. Chem. 69 (1965) 2950–2954.

[35] K.F. Wong, S. Ng, J. Chem. Soc. Faraday Trans. II 71 (1975) 622–630.
[36] B. Hilton, G.E. Martin, J. Nat. Prod. 73 (2010) 1465–1469.
[37] P.I. Nagy, A. Maheshwari, Y.-W. Kim, W.S. Messer Jr., J. Phys. Chem. B 114 (2010) 349–360.
[38] A. Lagutschenkov, J. Langer, G. Berden, J. Oomens, O. Dopfer, J. Phys. Chem. A 114 (2010) 13268–13276.
[39] F.A.L. Anet, I. Yavari, Org. Magn. Reson. 12 (1979) 362–364.
[40] A.T. Bottini, J.D. Roberts, J. Am. Chem. Soc. 78 (1956) 5126.
[41] M. Saunders, F. Yamada, J. Am. Chem. Soc. 85 (1963) 1882.
[42] D. de Loera, F. Liu, K.N. Houk, M.A. Garcia-Garibay, J. Org. Chem. 78 (2013) 11623–11626.
[43] A.M. Belostotskii, H.E. Gottlieb, P. Aped, A. Hassner, Chem. Eur. J. 5 (1999) 449–455.
[44] J.E. Anderson, D. Cazarini, J.E.T. Corrie, L. Lunazzi, J. Chem. Soc. Perkin Trans. 2 (1993) 1299–1304.
[45] H. Kessler, Angew. Chem. 82 (1970) 237–253.
[46] M.D. Pluth, R.G. Bergman, K.N. Raymond, J. Am. Chem. Soc. 130 (2008) 6362–6366.
[47] J.H. Poupaert, F.A. Gbaguidi, C.N. Kapanda, H. Aichaoui, C.R. McCurdy, Med. Chem. Res. 22 (2013) 247–252.
[48] R. Glaser, Q.-J. Peng, A.S. Perlin, J. Org. Chem. 53 (1988) 2172–2180.
[49] J.C. Wilson, S.L.A. Munro, D.J. Craik, Magn. Reson. Chem. 33 (1995) 367–374.
[50] W.R. Morgan, D.E. Leyden, J. Am. Chem. Soc. 92 (1970) 4527–4531.
[51] M. Ōki, M. Ohira, Y. Yoshioka, T. Morita, H. Kihara, N. Nakamura, Bull. Chem. Soc. Jpn. 57 (1984) 2224–2229.
[52] G. Bifulco, R. Riccio, G.E. Martin, A.V. Buevich, R.T. Williamson, Org. Lett. 15 (2013) 654–657.
[53] D.R. Lide (Ed.), CRC Handbook of Chemistry and Physics, 69th ed., CRC press, Boca Raton, Fl, 1988 p. C-498.
[54] P.L. Polavarapu, A. Petrovic, F. Wang, Chirality 15 (2003) S143–S149.
[55] P.J. Stephens, D.M. McCann, J.R. Cheeseman, M.J. Frisch, Chirality 17 (2005) S52–S64.
[56] J. Kongsted, K. Ruud, Chem. Phys. Lett. 451 (2008) 226–232.
[57] B. Mennucci, C. Cappelli, R. Cammi, J. Tomasi, Chirality 23 (2011) 717–729.
[58] A. Shimizu, T. Mori, Y. Inoue, S. Yamada, J. Phys. Chem. A 113 (2009) 8754–8764.
[59] J.W. Snow, T.M. Hooker, Can. J. Chem. 56 (1978) 1222–1230.
[60] V. Setnička, M. Urbanová, S. Pataridis, V. Král, K. Volka, Tetrahedron Asymmetry 13 (2002) 2661–2666.
[61] V.A. Narayanan, N.A. Stump, G.D. Del Cul, T. Vo-Dinh, J. Raman Spectrosc. 30 (1999) 435–439.
[62] Gaussian09, M.J. Frisch, et al., Gaussian 09, Gaussian, Inc., Wallingford CT, 2009. RevA.02.
[63] C. Adamo, V. Barone, J. Chem. Phys. 108 (1998) 664–675.
[65] E.R. Davidson, Chem. Phys. Lett. 260 (1996) 514–518.
[64] T.H. Dunning Jr., J. Chem. Phys. 90 (1989) 1007–1023.